Article

Fe-Labeled Octamethylferrocenium Tetrafluoroborate. X-ray Crystal Structures of Conformational Isomers, Hyperfine Interactions, and Spin–Lattice Relaxation by Moessbauer Spectroscopy

Herwig Schottenberger, Klaus Wurst, Ulrich J. Griesser, Ram K. R. Jetti, Gerhard Laus, Rolfe H. Herber, and Israel Nowik

J. Am. Chem. Soc., **2005**, 127 (18), 6795-6801• DOI: 10.1021/ja050452h • Publication Date (Web): 15 April 2005

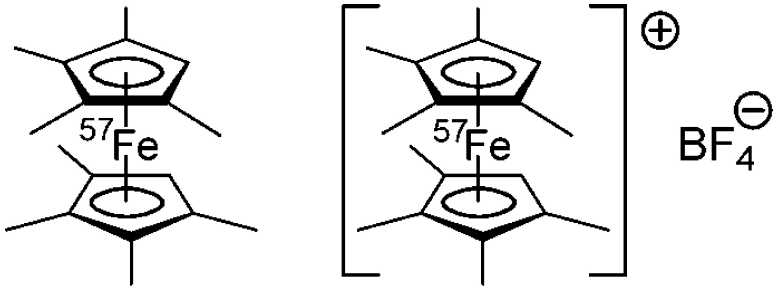

1 **2**

More About This Article

Additional resources and features associated with this article are available within the HTML version:

- Supporting Information
- Links to the 1 articles that cite this article, as of the time of this article download
- Access to high resolution figures
- Links to articles and content related to this article
- Copyright permission to reproduce figures and/or text from this article

View the Full Text HTML

J|A|C|S
ARTICLES
Published on Web 04/15/2005

^{57}Fe-Labeled Octamethylferrocenium Tetrafluoroborate. X-ray Crystal Structures of Conformational Isomers, Hyperfine Interactions, and Spin−Lattice Relaxation by Moessbauer Spectroscopy

Herwig Schottenberger,*,† Klaus Wurst,† Ulrich J. Griesser,† Ram K. R. Jetti,† Gerhard Laus,*,‡ Rolfe H. Herber,*,§ and Israel Nowik

Contribution from the Faculty of Chemistry and Pharmacy, University of Innsbruck, 6020 Innsbruck, Austria, Immodal Pharmaka GmbH, 6111 Volders, Austria, and The Racah Institute of Physics, The Hebrew University of Jerusalem, 91904 Jerusalem, Israel

Received January 23, 2005; E-mail: herwig.schottenberger@uibk.ac.at; g.laus@gmx.net; herber@vms.huji.ac.il

Abstract: X-ray structure determinations of two different single crystals of octamethylferrocenium tetrafluoroborate ($OMFc^+BF_4^-$) revealed conformational polymorphism with ligand twist angles of 180° and 108°, respectively. Their concomitant occurrence could be explained by the small lattice energy difference of 3.2 kJ mol^{-1}. Temperature-dependent Moessbauer spectroscopy of ^{57}Fe-labeled $OMFc^+BF_4^-$ over the range $90 < T < 370$ K did not show the anomalous sudden increase in the motion of the metal atom as observed in neutral OMFc. Broadened absorption curves characteristic of relaxation spectra were obtained with an isomer shift of 0.466(6) mm s^{-1} at 90 K. The temperature dependence of the isomer shift corresponded to an effective vibrating mass of 79 ± 10 Da and, in conjunction with the temperature dependence of the recoil-free fraction, to a Moessbauer lattice temperature of 89 K. The spin relaxation rate could be better described by an Orbach rather than a Raman process. At 400 K, a reversible solid−solid transition to a plastic crystalline mesophase was noted.

Introduction

Static and dynamic structures of organometallic molecules have drawn broad interest in the booming field of materials chemistry.[1] Especially ferrocenes represent a large model pool for basic research due to their exceptional chemical stability and their structural diversity. Therefore, ferrocenes are one of the most promising groups of compounds to connect both fields of applied and basic research. The librational motion, ring orientation and rotation, and phase transition phenomena in ferrocene have been extensively reviewed in the recent literature.[2] The connections between polymorphism, structure−property relations, and crystal growth have been discussed.[3] In particular, organometallic polymorphism[4] involving conformationally flexible metallocenes often gives rise to different rotamers with regard to the relative orientation of the cyclopentadienide (Cp) rings. Molecular structures of polyalkylmetallocenes are usually probed by several different, complementary techniques. Thus, conformational properties of 1,1′-di-*tert*-butylferrocene were examined by X-ray diffraction, gas-phase electron diffraction, and theoretical calculations of ring rotation energy profiles.[5] Moreover, it is interesting to compare neutral and cationic species. Crystal structures of sterically congested hexa- and octa-*iso*-propylmetallocenes and the corresponding metallocenium salts have been reported.[6] In particular, the reported crystal structures of octamethylferrocene (OMFc; **1**) revealed a staggered conformation with a ligand twist angle of 180° (space groups $P2(1)/n$[7] and $P2(1)c$[8]), whereas the cation in the $OMFc^+PF_6^-$ salt adopts an almost eclipsed conformation with a twist angle of 8.7° (space group $C2/c$).[9] In other salts, $OMFc^+$ cations have been found in staggered conformations.[10] It is also noteworthy that unusual magnetic behavior of decamethylferrocene (DMFc) charge-transfer salts has been associated with different structural phases.[11]

† University of Innsbruck.
‡ Immodal Pharmaka GmbH.
§ The Hebrew University of Jerusalem.

(1) Braga, D.; Grepioni, F. In *Topics in Organometallic Chemistry*; Brown, J. M., Hofmann, P., Eds.; Springer: Berlin, Heidelberg, 1999; pp 47−68.
(2) (a) Braga, D. *Chem. Rev.* **1992**, *92*, 633. (b) Dunitz, J. D. *Acta Crystallogr., Sect. B* **1995**, *51*, 619. (c) Brock, C. P.; Fu, Y. *Acta Crystallogr., Sect. B* **1997**, *53*, 928. (d) Calvarin, G.; Clec'h, G.; Berar, J. F.; Amndre, D. *J. Phys. Chem. Solids* **1982**, *43*, 785. (e) Takusasawa, F.; Koetzle, T. F. *Acta Crystallogr., Sect. B* **1979**, *35*, 1074.
(3) Bernstein, J. *J. Phys. D: Appl. Phys.* **1993**, *26*, B66.
(4) Braga, D.; Grepioni, F. *Chem. Soc. Rev.* **2000**, *29*, 229.
(5) Morrison, C. A.; Bone, S. F.; Rankin, D. W. H.; Robertson, H. E.; Parsons, S.; Coxall, R. A.; Fraser, S.; Howell, J. A. S.; Yates, P. C.; Fey, N. *Organometallics* **2001**, *20*, 2309.
(6) Burkey, D. J.; Hays, M. L.; Duderstadt, R. E.; Hanusa, T. P. *Organometallics* **1997**, *16*, 1465.
(7) Struchkov, Y. T.; Andrianov, V. G.; Salnikova, T. N.; Lyatifov, I. R.; Materikova, R. B. *J. Organomet. Chem.* **1978**, *145*, 213.
(8) Schmitz, D.; Fleischhauer, J.; Meier, U.; Schleker, W.; Schmitt, G. *J. Organomet. Chem.* **1981**, *205*, 381.
(9) Andrianov, V. G.; Struchkov, Yu. T.; Lyatifov, I. R.; Materikova, R. B. *Koord. Khim.* **1982**, *8*, 846.
(10) Miller, J. S.; Glatzhofer, D. T.; O'Hare, D. M.; Reiff, W. M.; Chakraborty, A.; Epstein, A. J. *Inorg. Chem.* **1989**, *28*, 2930.
(11) (a) Wang, G.; Slebodnik, C.; Butcher, R. J.; Tam, M. C.; Crawford, T. D.; Yee, G. T. *J. Am. Chem. Soc.* **2004**, *126*, 16890. (b) Broderick, W. E.; Eichhorn, D. M.; Liu, X.; Toscano, P. J.; Owens, S. M.; Hoffman, B. M. *J. Am. Chem. Soc.* **1995**, *117*, 3641.

Chart 1

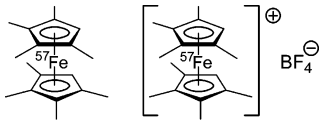

1 2

Recent variable-temperature ^{57}Fe Moessbauer spectroscopic studies have elucidated the unusual metal atom dynamics in OMFc[12] and related organometallics.[13] In particular, it was shown that while the temperature dependence of the logarithm of the recoil-free fraction, ln *f*, is reasonably linear in the range $90 \leq T \leq 347$ K, the resonance effect abruptly becomes vanishingly small above 350 K, that is some 80 °C below the melting point, T_{mp}. This phenomenon was ascribed to the effect of librational motion of the ligands concurrent with the onset of ring rotation in the solid and is consistent with differential scanning calorimetry results (DSC) for OMFc.[12] This librational degree of freedom, in turn, results in a large increase in the mean-square-amplitude-of-vibration *msav* of the metal atom with its associated effect on *f*. Similar effects have been documented in the case of nonamethylferrocene (NMFc),[14,15] ethynyl OMFc,[16,17] and ethenyl OMFc,[18] but were absent in ionic oxidation products ($NMF^+PF_6^-$ and ethynyl $OMFc^+PF_6^-$) and in compounds with longer, more polar side chains such as 2-nitro-3-(OMFc)acrylonitrile[19] and (OMFc)methylenemalononitrile.[20] This anomalous metal motion was also absent in the case of the highly symmetrical DMFc.[21] It is noteworthy that this onset of motion below room temperature is also reflected by the observation that no resolvable X-ray structures of NMFc[15] and ethynyl OMFc[16] single crystals could be obtained at ambient temperature.

When diamagnetic iron-organometallics are subjected to one-electron oxidation, the normal Moessbauer spectrum of the former, which consists of two well-separated components of the quadrupole split (*Q.S.*) absorbance, is replaced by an absorption spectrum that consists of an asymmetric broad line that can be associated with spin−lattice relaxation of the unpaired electron in the paramagnetic oxidation product. The fundamental theoretical treatment of this *Q.S.* "collapse" was reported in a classical study by Collins.[22] Accordingly, Moessbauer spectroscopy has been employed to monitor intramolecular electron-transfer processes[23] and mixed-valence species[24] involving ferrocenes.

(12) Nowik, I.; Herber, R. H. *Inorg. Chim. Acta* **2000**, *310*, 191.
(13) Schottenberger, H.; Buchmeiser, M.; Herber, R. H. *J. Organomet. Chem.* **2000**, *612*, 1.
(14) Herber, R. H. In *Unusual Structures and Physical Properties in Organometallic Chemistry*; Gielen, M., Willem, R., Wrackmeyer, B., Eds.; J. Wiley and Sons: West Sussex, 2002; pp 211−214.
(15) Herber, R. H.; Nowik, I.; Schottenberger, H.; Wurst, K.; Schuler, N.; Müller, A. G. *J. Organomet. Chem.* **2003**, *682*, 163.
(16) Schottenberger, H.; Wurst, K.; Herber, R. H. *J. Organomet. Chem.* **2001**, *625*, 200.
(17) Herber, R. H.; Nowik, I. *Hyperfine Interact.* **2000**, *126*, 127.
(18) (a) Herber, R. H.; Nowik, I. *Hyperfine Interact.* **2002**, *141/142*, 297. (b) Herber, R. H. In *Unusual Structures and Physical Properties in Organometallic Chemistry*; Gielen, M., Willem, R., Wrackmeyer, B., Eds.; J. Wiley and Sons: West Sussex, 2002; pp 214−216.
(19) Laus, G.; Schottenberger, H.; Schuler, N.; Wurst, K.; Herber, R. H. *J. Chem. Soc., Perkin Trans. 2* **2002**, 1445.
(20) Laus, G.; Schottenberger, H.; Wurst, K.; Herber, R. H.; Griesser, U. *J. Phys. Chem. B* **2004**, *108*, 5082.
(21) Herber, R. H. *Inorg. Chim. Acta* **1999**, *291*, 74.
(22) Collins, R. L. *J. Chem. Phys.* **1964**, *42*, 1072.
(23) Ratera, I.; Ruiz-Molina, D.; Renz, F.; Ensling, J.; Wurst, K.; Rovira, C.; Gütlich, P.; Veciana, J. *J. Am. Chem. Soc.* **2003**, *125*, 1462.
(24) Jiao, J.; Long, G. J.; Grandjean, F.; Beatty, A. M.; Fehlner, T. P. *J. Am. Chem. Soc.* **2003**, *125*, 7522.

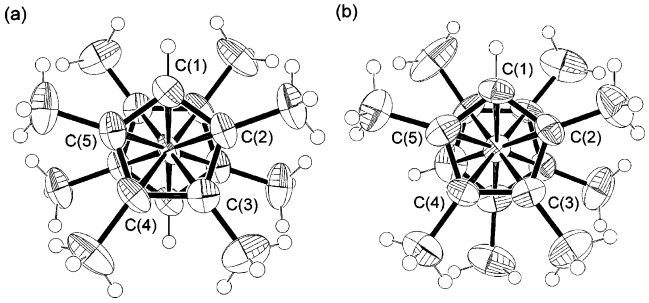

Figure 1. ORTEP plots showing the conformation of the two rotational isomers of the OMFc cation in the crystal structures of $OMFc^+BF_4^-$ (**2**), with ligand twist angles of (a) 180° in **2a** and (b) 108° in **2b** (displacement ellipsoids are drawn at the 50% probability level).

Because both the *f*(*T*) behavior as well as the temperature dependence of the spin−lattice relaxation rate are expected to be sensitive to the molecular level architecture of OMFc (**1**) and $OMFc^+BF_4^-$ (**2**) (Chart 1), it was considered desirable to examine these dependences in some detail. In an earlier study,[12] both spin−lattice relaxation and recoil-free fraction data have been reported for $OMFc^+PF_6^-$ [65253-91-0], but because these data were acquired with natural abundance ^{57}Fe material, little statistically significant information could be extracted from the high-temperature data. Because *f* becomes very small with the onset of ring rotation, it was necessary to prepare ^{57}Fe-labeled $OMFc^+$ to study this effect to a greater extent in the neighborhood of the dynamical anomaly, and the present study reports the details of the preparation of this labeled material as well as the information extracted from a careful Moessbauer study of this product.

Results and Discussion

A. X-ray Structure Determination of Conformational Isomers. In the reported structure of the $OMFc^+PF_6^-$ salt,[9] the cation adopts an almost eclipsed conformation with a ligand twist angle of 8.7°. In search for other conformers, the BF_4^- salt was prepared, and single crystals were obtained from solutions in dichloromethane at room temperature. As was hoped, this compound exhibited conformational polymorphism, and two different types of crystals **2a** and **2b** were observed. Their molecular structures are shown in Figure 1. The cation in crystal **2a** possesses a crystallographically imposed center of inversion at the iron atom, with a ring centroid−Fe distance of 1.7086 Å and a ring normal−Fe distance of 1.7080(11) Å. Figure 2a shows the crystal structure of **2a**, which crystallizes in the space group *C*2/*c*. In the crystal, the inversion-related cations stack along the *c*-axis forming columns. The adjacent columns along the *b*-axis are filled by BF_4^- anions involving weak C−H···F interactions[25] (less than the van der Waals radii) leading to a perfectly parallel columnar arrangement. In contrast, in crystal **2b** a different orientation of the ligands was found, with the Cp rings being twisted by approximately 108°. The deviation from regular pentagon is more pronounced in one of the rings, C(1), having the shortest Fe distance and the largest ring angle. Ring centroid−Fe distances are 1.7005 and 1.7088 Å, and ring normal−Fe distances are 1.6996(31) and 1.7084(29) Å. The rings are slightly nonparallel (ring centroid−Fe−ring centroid angle 179.13°) with a dihedral tilt angle of 1.9(3)°.

(25) Desiraju, G. R.; Steiner, T. *The Weak Hydrogen Bond in Structural Chemistry and Biology*; Oxford University Press: Oxford, 1999.

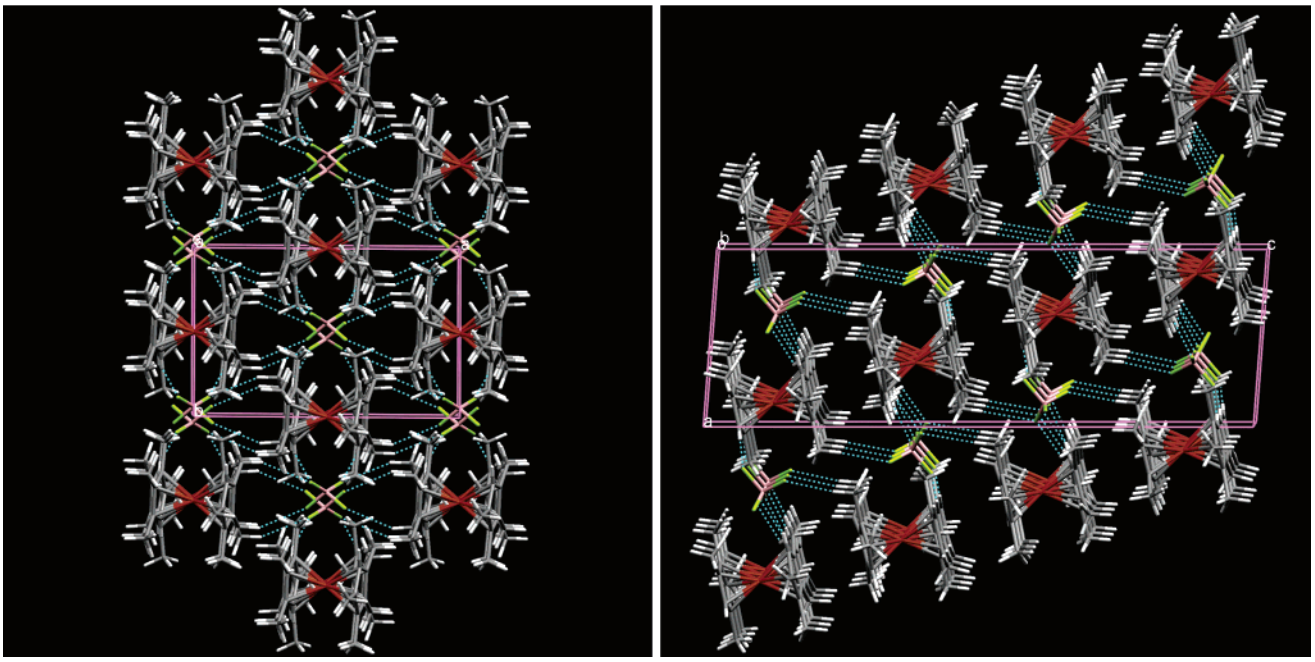

Figure 2. (a) Crystal structure of **2a**, view along the *c*-axis showing a perfect columnar arrangement. BF_4^- anions fill the gaps between the columns along the *b*-axis by weak C−H···F interactions. (b) Crystal structure of **2b**, view along the *b*-axis showing the off-stacked layer-type arrangement. These layers are based on weak C−H···F interactions along the *a*-axis. The BF_4^- anions are disordered in both forms, and only one of the disorder positions is shown for clarity.

Table 1. Crystal Data and Structure Refinement for the Conformational Isomers **2a** and **2b** of $OMFc^+BF_4^-$

	2a	**2b**
molecular formula	$C_{18}H_{26}BF_4{}^{57}Fe$	$C_{18}H_{26}BF_4{}^{57}Fe$
M_r	385.05	385.05
crystal system	monoclinic	monoclinic
space group	*C*2/*c*	*P*2(1)/*n*
a, Å	13.6067(9)	8.4000(10)
b, Å	8.1374(4)	8.5030(10)
c, Å	17.5031(9)	25.916(4)
β, deg	109.835(3)	94.353(6)
V, Å^3	1823.02(18)	1845.7(4)
Z	4	4
T, K	233(2)	233(2)
D_{calcd}, g cm^{-3}	1.403	1.386
μ, mm^{-1}	0.861	0.851
F(000)	804	804
color, habit	green plate	green plate
crystal dimensions, mm	0.4 × 0.4 × 0.04	0.31 × 0.17 × 0.03
θ range for data collection, deg	2.47−22.97	2.50−20.49
index ranges	$0 \le h \le 14$ $-8 \le k \le 8$ $-19 \le l \le 18$	$0 \le h \le 8$ $-8 \le k \le 8$ $-25 \le l \le 25$
reflections collected	4426	6301
independent reflections	1266 (R_{int} = 0.0265)	1855 (R_{int} = 0.1039)
reflections with $I > 2\sigma(I)$	1068	1186
data/restraints/parameters	1266/0/133	1855/0/261
goodness-of-fit on F^2	1.053	0.971
final *R* indices [$I > 2\sigma(I)$]	R_1 = 0.0310, wR_2 = 0.0796	R_1 = 0.0578, wR_2 = 0.1261
R indices (all data)	R_1 = 0.0395, wR_2 = 0.0828	R_1 = 0.1066, wR_2 = 0.1414

Figure 2b shows the crystal structure of **2b**, which crystallizes in the space group $P2_1/n$. The structure is similar to **2a** in forming columns involving inversion-related stacks of the cations. However, the adjacent columns **2b** along the *a*-axis are offset and connected by BF_4^- anions in a side-on way by weak C−H···F interactions forming a layerlike structure. The F-atoms of the BF_4^- anion in both **2a** and **2b** are disordered over two sites with occupancies of 0.5 each. Crystallographic data and details of the refinement are summarized in Table 1. Selected bond lengths and angles are given in the Supporting Information.

To our knowledge, these are the first examples of simultaneously crystallizing metallocene rotamers. Obviously, these crystal structures are energetically nearly equivalent, a phenomenon that has been termed "concomitant polymorphism".[26] This was further confirmed by lattice energy calculations. The data in Table 2 show that **2a** is more stable than **2b** by 3.2 kJ mol^{-1} due to stronger electrostatic interactions. The small energy difference between the two forms also hints to the concomitant

(26) Bernstein, J.; Davey, R. J.; Henck, J.-O. *Angew. Chem., Int. Ed.* **1999**, *38*, 3440.

Table 2. Lattice Energy Calculations of the Polymorphs **2a** and **2b** of $OMFc^+BF_4^-$ (Energy Contributions per mol)

energy contribution	**2a** kJ mol^{-1}	**2b** kJ mol^{-1}
van der Waals	−41.80	−48.30
electrostatic	−112.70	−101.97
hydrogen bond	−8.42	−9.45
total energy	−162.93	−159.74

nature of these polymorphs, which were obtained from the same crystallization flask.

B. X-ray Powder Diffraction and Thermochemical Behavior. Apart from the single crystals, it was of interest to investigate the conformational nature of the microcrystalline bulk $OMFc^+BF_4^-$, which had been prepared by precipitation. Figure 3 shows the X-ray powder patterns of both conformers calculated from the crystal structures in comparison with the experimental powder pattern of precipitated $OMFc^+BF_4^-$. The experimental pattern of this sample matched well with that calculated for **2b**, displaying Bragg reflections at *d* values of 7.80, 7.10, 6.46, 5.88, 4.79, 4.25, 4.08, 3.55, and 3.48 Å (2θ values of 11.3°, 12.5°, 13.7°, 15.0°, 18.5°, 20.9°, 21.8°, 25.1°, and 25.6°). Obviously, it can be concluded that the $CpMe_4$ rings in the precipitated bulk material adopt the conformation with the twist angle of 108°.

Hot stage microscopy showed that the crystals of **2b** exhibit a solid−solid phase transition at about 400 K. The transformation can be easily recognized by the loss of birefringence indicating the transformation to a cubic crystal. This high symmetry points at the formation of a plastic crystalline mesophase,[27] assuming that the OMFc molecules start to tumble above the transition temperature as if they were in solution. Such phases are often referred to as rotator phases.[28] Preliminary DSC experiments indicated rather high enthalpy and entropy of transition values ($\Delta_{trs}H \approx 9$ kJ mol^{-1}, $\Delta_{trs}S \approx 30$ J mol^{-1} K^{-1}), which lie in the expected range of such a phase transition. The transition is reversible and occurs on cooling at about 380 K. This reversibility is a further characteristic of plastic crystalline phases. The X-ray powder pattern of the cubic crystals recorded at 413 K (Figure 3) shows only four distinct Bragg reflections at *d* values of 7.34, 6.34, 4.48, and 3.66 Å (2θ values of 12.1°, 14.0°, 19.8°, and 24.3°) due to the reorganization of the lattice. Similar order−disorder transitions have also been reported for other ferrocenes such as ethynyl OMFc,[29] ferrocenium PF_6^-,[30] 1,1′,2,2′-tetrachloroferrocene,[31] and ferrocene carbaldehyde.[32] At higher temperatures the crystals start to decompose, making it impossible to determine the final melting point.

C. Hyperfine Interactions. The temperature dependence of the isomer shift *I.S.* in the high-temperature regime ($296.6 \leq T \leq 370$ K) is well fitted by a linear correlation with $r = 0.96$ for 10 data points. From this temperature dependence,[33] the effective vibrating mass M_{eff} is 79 ± 10 Da, somewhat smaller than the corresponding value for **1** (98 Da). It is worthwhile noting that the *I.S.* of **2b** is smaller than that of **1** by ∼0.037 mm s^{-1} at 90 K. This decrease can be related to the fact that the metal−ligand interaction involves an overlap between the metal 3d orbitals and the π-electrons of the Cp ring. Formal removal of 3d electron density on oxidation decreases the shielding of the s-electron density at the Fe nucleus. This decrease in shielding, in turn, increases the s-electron density, and hence decreases the *I.S.*, as observed. Similar effects have been repeatedly noticed in related iron−organometallic systems.[12,14,16]

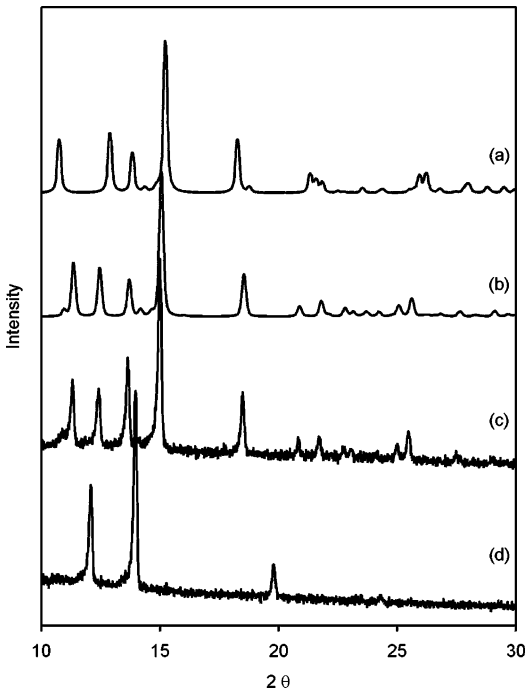

Figure 3. Calculated X-ray powder diffraction patterns for the conformational isomers (a) **2a**, (b) **2b**, and experimental data of (c) precipitated $OMFc^+BF_4^-$ **2b** at 296 K, and of (d) cubic crystals derived from **2b** at 413 K.

The temperature dependence of ln *f* for **2b**, as reflected in the logarithm of the area under the resonance curve, is again well fitted by a linear correlation in the high-temperature regime, with $r = 0.99$ for 10 data points, and is summarized graphically in Figure 4.

This dependence, together with that of the *I.S.*, leads to a Moessbauer lattice temperature,[33] θ_M (as probed by the iron atom), of 89 ± 5 K. In this context, it is worthwhile noting that in contrast to the temperature dependence of ln *f* for **1**, which shows a sudden drastic diminution at $T > 348$ K, the resonance effect in **2b** is still readily observable with the ^{57}Fe-enriched sample at $T \geq 370$ K. The logical inference from this observation is that strong electrostatic interactions due to the presence of charged species in the lattice inhibit the onset of rotation of the η^5-$CpMe_4$ ring and thus the participation of librational modes affecting the iron atom motion. The hyperfine parameters of **2b** and related compounds, together with derived and related parameters, are summarized in Table 3. In the high-temperature regime, the *Q.S.* parameter (∼ ∠0.11 mm s^{-1}) is essentially temperature independent.

(27) (a) Sherwood, J. N., Ed. *The plastically crystalline state (orientationally disordered crystals)*; Wiley: Chichester, 1979. (b) Parsonage, N. G.; Staveley, L. A. K. *Disorder in Crystals*; Clarendon Press: Oxford, 1978.
(28) MacFarlane, D. R.; Meakin, P.; Amini, N.; Forsyth, M. *J. Phys.: Condens. Matter* **2001**, *13*, 8257.
(29) Asthalter, T.; Franz, H.; van Burck, U.; Messel, K.; Schreier, E.; Dinnebier, R. *J. Phys. Chem. Solids* **2003**, *64*, 677.
(30) Webb, R. J.; Lowery, M. D.; Shiomi, Y.; Sorai, M.; Wittebort, R. J.; Hendrickson, D. N. *Inorg. Chem.* **1992**, *31*, 5211.
(31) Uchimi, F. Y.; Masuda, Y.; Iwai, K.; Katada, M.; Sano, H. *Hyperfine Interact.* **1988**, *42*, 1091.
(32) Makarov, E. F.; Rochev, V. Ya.; Kevdin, O. P.; Kukushkina, L. B. *Khim. Fiz.* **1985**, *4*, 1532.
(33) Herber, R. H. In *Chemical Mössbauer Spectroscopy*; Herber, R. H., Ed.; Plenum Press: New York, 1984; pp 199−216.

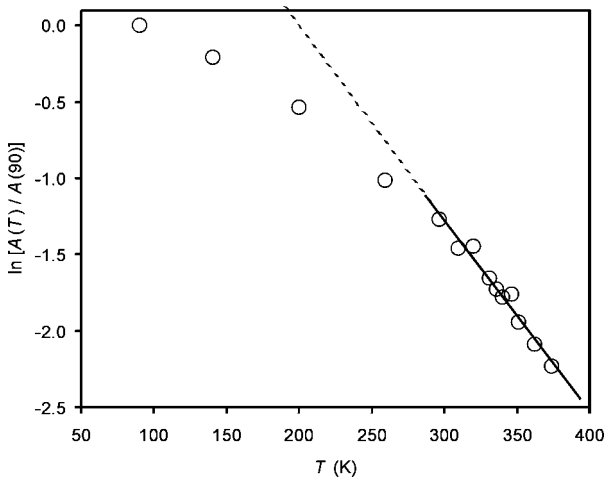

Figure 4. Temperature dependence of the Moessbauer recoil-free fraction (as reflected in the logarithm of the normalized area values) for the title compound **2b**. From the high-temperature limiting slopes of the isomer shift and recoil-free fraction data, the calculated value of θ_M is 89 ± 5 K.

In this context, it is interesting to note that the temperature dependences of ln *f* in the low *T* region for both the BF_4^- salt ($-4.23(1) \times 10^{-3}$ K^{-1}; $r = 0.938$ for 12 data points] and the PF_6^- salt ($-5.65(5) \times 10^{-3}$ K^{-1}; $r = 0.990$ for 13 data points) are both somewhat smaller than that for the neutral parent compound in the low-temperature regime (90−300 K) ($-7.21(22) \times 10^{-3}$ K^{-1}; $r = 0.996$ for 8 data points), indicating the expected "stiffer" salt lattice. Table 3 includes, in addition to the data pertaining to **1** and **2b**, the corresponding parameters for nonamethylferrocene (NMFc) and its PF_6^- salt, as well as for DMFc and its PF_6^- and BF_4^- salts, for comparison purposes. Moreover, it should be noted that individual temperature regimes have been noted because both low- and high-temperature regimes must be considered in each case, as is illustrated in Figure 4. Some of these data have been previously reported in detail.[14]

D. Spin Relaxation in Octamethylferrocene Tetrafluoroborate and Related Organometallics. The broad asymmetric absorption recorded at 90 K decreases markedly in width as the temperature is raised to 370 K. This narrowing is the result of the spin−lattice relaxation rate temperature dependence. The details of the resonance absorption are characteristic of iron compounds, which show spin−lattice relaxation on a time scale comparable to that of the 14.4 keV transition in ^{57}Fe. Moessbauer spectroscopic observations of paramagnetic spin relaxation phenomena are common for ionic, trivalent compounds but much less so for divalent, predominantly covalent homologues.[34] The spectra are, in most cases, analyzed in terms of a fluctuating effective magnetic hyperfine field corresponding to the ionic doublet ground state. In trivalent iron compounds, the hyperfine field is generally around 500 kOe (such as for the $S_z = \pm^5/_2$ state of pure Fe^{3+}). In ferrocene and related compounds, the iron is held by both covalent (∼50%) and ionic bonds[35] and is diamagnetic. When subjected to one-electron oxidation, it becomes paramagnetic, with an effective spin of $^1/_2$.[36] The fluctuating magnetic hyperfine field cannot be determined, because even at 4.2 K the spectra do not have a well-resolved magnetic structure, probably due to temperature-independent spin−spin relaxation. In the absence of more detailed information, the present data have been arbitrarily analyzed in terms of a fluctuating magnetic hyperfine field of $H_{int} = 500$ kOe. The high relaxation rates obtained for the ferrocene systems are easily adjusted for any other hyperfine field, and the rate should vary in proportion with the square of H_{int}.[37]

The observed temperature dependence of the spin relaxation rate ($1/\tau$) can be compared to theoretical predictions for a ground-state paramagnetic doublet.[38] In the case of $OMFc^+PF_6^-$, the spin relaxation rates were analyzed in terms of a temperature power law, and reasonable agreement was obtained with a $T^{2.2}$ dependence in the range $90 < T < 300$ K.[12] In trying to fit several other systems with such a power law, the success was much more limited. It was found that a formula corresponding to the Orbach process[39] agrees much better with the experimental observations. Thus, the relaxation rate temperature dependences measured in this study were fitted using a relationship of the form (eq 1)

$$1/\tau = r_{ss} + r_o/(\exp(\Delta/k_BT) - 1) \qquad (1)$$

where r_{ss} corresponds to the spin−spin relaxation rate, r_o corresponds to an Orbach relaxation rate, and Δ is the energy of the first excited state above the iron ground doublet state. In the present cases, this state is the first excited molecular level.[40] The relative contribution of spin−spin relaxation in the temperature ranges here reported plays only a minor role. A representative data set for the temperature dependence of τ for $OMFc^+BF_4^-$ (**2b**) is summarized graphically in Figure 5.

The solid line in Figure 5 is the result of a nonlinear curve fitting procedure using a Levenberg−Marquardt iteration method and corresponds to the temperature dependence given by the Orbach process in the above eq 1. For $OMFc^+BF_4^-$, $r_o = 15 \times 10^{12}$ s^{-1}, $r_{ss} = 22 \times 10^9$ s^{-1}, and $\Delta/k_B = 1690$ K (0.15 eV; 1174 cm^{-1}; 14.2 kJ mol^{-1}). It is also evident from this figure that, as in the case of the recoil-free fraction data, there is no persuasive evidence for a discontinuity in the data at ∼350 K, the temperature at which *f* for the neutral compound becomes experimentally unobservable. Comparable spin−lattice relaxation data have been acquired for the PF_6^- salt,[12] but the data there were limited to the temperature range $90 < T < 300$ K due to the fact that only natural abundance ^{57}Fe material was available for study. For this compound, over the above temperature range, the Orbach process relationship also fits the data better than a power law dependence. In this context, it is also worthwhile noting that in the case of $DMFc^+PF_6^-$ [54182-44-4],[41] the temperature dependence of the spin−lattice relaxation rate was also fit by the Orbach process eq 1 with $r_o = 6.9 \times 10^{12}$ s^{-1}, $r_{ss} = 5.8 \times 10^9$ s^{-1}, and $\Delta/k_B = 1134$ K (0.10 eV;

(34) (a) Wickman, H. H.; Wetheim, G. K. In *Chemical Applications of Mössbauer Spectroscopy*; Goldanskii, V. I., Herber, R. H., Eds.; Academic Press: New York, 1968; Chapter 11 and references therein. (b) Greenwood, N. N.; Gibb, T. C. In *Mössbauer Spectroscopy*; Chapman Hall Ltd.: London, 1971; pp 72−74 and references therein.
(35) Frenking, G. *J. Organomet. Chem.* **2001**, *635*, 9.
(36) Herber, R. H.; Nowik, I.; Loginov, D. A.; Starikova, Z. A.; Kudinov, A. R. *Eur. J. Inorg. Chem.* **2004**, 3476.
(37) (a) Nowik, I. *Hyperfine Interact.* **1983**, *13*, 89. (b) Abragam, A. *Principles of Nuclear Magnetism*; Clarendon Press: Oxford, 1961; pp 447−451.
(38) Abragam, A.; Bleany, B. *Electron Paramagnetic Resonance of Transition Ions*; Clarendon Press: Oxford, 1970; pp 560−561.
(39) (a) Finn, C. B. P.; Orbach, R.; Wolf, W. P. *Proc. Phys. Soc.* **1961**, *77*, 261. (b) For a detailed discussion, see ref 38.
(40) Baik, M.-H.; Crystal, J. B.; Friesner, R. A. *Inorg. Chem.* **2002**, *41*, 5926.
(41) (a) Herber, R. H.; Hanusa, T. P. *Hyperfine Interact.* **1997**, *108*, 563. (b) Cohn, M. J.; Timken, M. D.; Hendrickson, D. N. *J. Am. Chem. Soc.* **1984**, *106*, 6683.

Table 3. Moessbauer Data for the Compounds Discussed in the Text[a]

compound	units	OMFc	$OMFc^+BF_4^-$	$OMFc^+PF_6^-$	NMFc	$NMFc^+PF_6^-$	DMFc	$DMFc^+PF_6^-$	$DMFc^+BF_4^-$
I.S. (90)	mm s^{-1}	0.520(3)	0.466(6)	0.491(13)	0.498(5)	0.492(7)	0.502(5)	0.460(15)	0.465(18)
Q.S. (90)	mm s^{-1}	2.571(5)	−0.291(6)	−0.192(13)	2.460(5)	−0.082(42)	2.479(5)	−0.189(15)	−0.362(18)
$-d\,I.S./dT$	10^{-4} mm s^{-1} K^{-1}	3.40(13)[b]	5.07(22)[d]	3.55(27)[g]	4.16(7)[i]	3.8(8)[k]	5.07(9)[m]	3.82(8)[o]	4.64(22)[p]
$-d\ln A/dT$	10^{-3} K^{-1}	7.21(22)[c]	not linear 4.23(1)[e] 12.4(4)[f]	5.65(5)[h]	8.57(19)[j]	not linear 15.9(6)[l]	not linear 16.1(3)[n]	not linear	not linear
$T_{\text{onset of libration}}$	K	∼350			∼260				
T_{mp}	K	431			480		567		

[a] The isomer shifts (*I.S.*) and quadrupole splitting (*Q.S.*) parameters at 90 K are indicated. The *I.S.* values refer to the centroid of an α-Fe spectrum at room temperature, which was also used for spectrometer calibration. The parenthetical numbers are the estimated errors in the last significant figures. Limited ranges over which temperature dependences were determined are given by footnotes as detailed below. [b] 90−300 K. [c] 90−300 K. [d] 260−370 K. [e] 90−200 K. [f] 297−370 K. [g] 85−298 K. [h] 86−300 K. [i] 170−290 K. [j] 85−210 K. [k] 90−335 K. [l] 210−335 K. [m] 230−370 K. [n] 250−370. [o] 90−360 K. [p] 110−273 K.

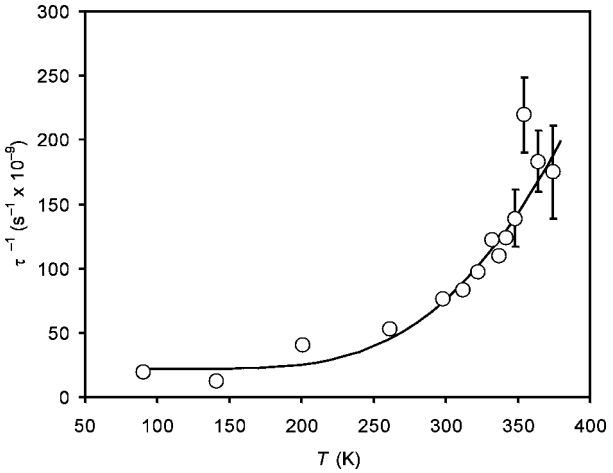

Figure 5. Relaxation rate τ^{-1} for the title compound **2b** as a function of temperature. The solid line is the result of Levenson−Marquardt iterations of the two-parameter function (eq 1) given in the text. The temperature regime above ∼300 K for the BF_4^- complex was experimentally accessible due to the use of the ^{57}Fe enriched material as described in the text.

788 cm^{-1}; 9.6 kJ mol^{-1}) in reasonable agreement with the data of the $OMFc^+$ salt cited above.

Conclusion

In the present work, different complementary techniques have been applied to elucidate the structure and the metal and ligand dynamics in solid $OMFc^+BF_4^-$. So far, three pairs of neutral and ionic polyalkylferrocenes have been available for variable-temperature Moessbauer spectroscopic studies in which the anomalous metal motion observed in the neutral compounds disappears upon oxidation. The sudden increase of metal motion in neutral OMFc, NMFc, ethenyl, and ethynyl OMFc is presumably due to the dynamical imbalance of the noncentrosymmetrically substituted Cp ligands, which imparts a wobbling librational/rotational movement. Facilitated by the use of ^{57}Fe-enriched material, which allows a higher temperature regime, Moessbauer spectroscopy again confirmed the absence of such an anomaly in a salt lattice. It is expected that substituents other than methyl contribute by electronic and not steric factors or, in other words, by the dipolarity of functional groups and not chain length. Thus, polar substituents are expected to create an environment similar to a salt lattice. Suitably tailored ^{57}Fe-labeled neutral model compounds with rigid but nonpolar substituents should provide further insight and proof of the concept presented here by exhibiting anomalous behavior. This should indicate how far steric and electronic contributions are responsible for the absence of the motion anomaly. Moreover, structural tailoring should allow addressing specifically the different kinds of motion, that is, spinning, wobbling, and tumbling. Finally, it should be possible to predict and subsequently verify the behavior of these planned probes into the dynamics of polyalkylferrocenes.

Experimental Section

Synthesis and Characterization. Enriched $^{57}FeCl_2$ was prepared from ^{57}Fe (95%, Advanced Materials Technologies, Israel) by a modified[15] literature procedure.[42] Labeled octamethylferrocene (**1**) was then prepared from $^{57}FeCl_2$ by complexation with the $CpMe_4$ anion[43] and oxidized with air in aqueous tetrafluoroboric acid to yield the cation **2** on a 50 mg scale.[44] The aqueous solution was repeatedly extracted with CH_2Cl_2, and the product **2b** was precipitated by addition of diethyl ether.

The elemental and isotopic composition of compounds **1** and **2** was determined by means of HR-MS (Finnigan MAT 95). The exact monoisotopic molecular weights were measured using the following conditions: (a) compound **1**, electron impact ionization (70 eV), resolution $R = 7000$, B-scan; average over 50 scans; (b) cation of BF_4^- salt **2**, LSIMS (Cs-gun, 20 kV, 2 μA, matrix: 3-nitrobenzyl alcohol), resolution $R = 9000$, E-scan, average over 50 scans.

OMFc (**1**): 299.1391; $C_{18}H_{26}{}^{57}Fe$ requires 299.1389. The determination of the ^{57}Fe/^{56}Fe isotope ratio of the starting compound **1** by means of HR-EI-MS ($R = 9000$, B-scan, average over 100 scans in HPROF-mode) gave a ^{57}Fe content of 95.0%.

$OMFc^+BF_4^-$ (**2**): 299.1375 (cation); $C_{18}H_{26}{}^{57}Fe$ requires 299.1389.

X-ray Structure Determination. Single crystals of **2a** and **2b** were obtained by slow evaporation of a saturated solution in dichloromethane at room temperature. The two different types of crystals were hand-picked. Diffraction data were measured on a Nonius Kappa CCD area-detector diffractometer using graphite-monochromated Mo Kα radiation ($\lambda = 0.71$ Å) with the detector placed 36 mm from the crystal via ϕ and ω-scans. Several scans in ϕ and ω directions were made to increase the number of redundant reflections, which were averaged in the refinement cycles. This procedure replaces an empirical absorption correction. The structures were solved by direct methods (SHELXS-86) and refined by full matrix least-squares against F^2 (SHELXL-93). All of the H-atom positions were generated by a riding model on idealized geometries with $U_{iso}(H) = 1.2\ U_{eq}(C)$ for the Cp rings or $U_{iso}(H) = 1.5\ U_{eq}(C)$ for the methyl groups. Details of the refinement and further crystallographic data are collected in Table 1. Crystallographic data for the structural analysis have been deposited with the Cambridge Crystallographic Data Centre, CCDC No. 249285 for **2a** and CCDC No. 249286 for **2b**.

(42) Aresta, M.; Nobile, C. F.; Petruzelli, D. *Inorg. Chem.* **1977**, *16*, 1817.
(43) Schmitt, G.; Özman, S. *Chem.-Ztg.* **1976**, *100*, 143.
(44) Nesmeyanov, A. N.; Materikova, R. B.; Lyatifov, I. R.; Kurbanov, T. K.; Kochetkova, N. S. *J. Organomet. Chem.* **1978**, *145*, 241.

X-ray Powder Diffraction. The experimental X-ray powder diffractogram was aquired with a Siemens D5000 diffractometer equipped with a θ/θ goniometer, a Cu Kα radiation ($\lambda = 1.54$ Å) source, a Goebel mirror (Bruker AXS), a 0.15° Soller slit collimator, and a scintillation counter. The pattern was recorded at a tube voltage of 40 kV and a tube current of 35 mA, applying a scan rate of 0.005° 2θ s^{-1} in the angular range of 2−40° 2θ. The program Powder Cell 2.3 was used for calculating the powder pattern from single-crystal data.[45]

Lattice Energy Calculations. The lattice energy calculations were carried out using the "crystal packer" module of the Cerius^2 package.[46] All molecules in the crystal were treated as rigid entries. Atom−atom potentials were estimated using a Dreiding 2.21 force field, and atomic charges were estimated using the charge equilibration method.

Moessbauer Spectroscopy. The Moessbauer spectrometer, its calibration, and the method of data reduction and thermal control have been described earlier.[47] The *I.S.* values are referred to the centroid of an α-Fe absorber spectrum at 298 K. A small contamination due to unoxidized neutral starting compound was observed, and its presence has been corrected for in the subsequent data analysis. The sample was shown by X-ray powder diffraction to consist only of type **2b** microcrystalline material.

Hot Stage Microscopy. The thermal behavior of $OMFc^+BF_4^-$ was observed with a Reichert Thermovar polarized light microscope equipped with a Kofler hot stage.

Acknowledgment. We are grateful to Prof. K.-H. Ongania (Institute of Organic Chemistry, University of Innsbruck) for the mass spectra. We thank Prof. T. Langer (Computer Aided Molecular Design Group, University of Innsbruck) for his help in the lattice energy calculations. R.K.R.J. acknowledges financial support from Lise-Meitner grant M862-B10 of the FWF.

Supporting Information Available: Crystallographic information files (CIF) and selected bond lengths and angles of the two conformational isomers of **2**. This material is available free of charge via the Internet at http://pubs.acs.org.

JA050452H

(45) Kraus, W.; Nolze, G. *Powder Cell for Windows*, Version 2.3; Federal Institute for Materials Research and Testing: Berlin, Germany, 1999.
(46) Cerius^2, Accelrys, Cambridge (U.K.). See www.accelrys.com.
(47) Herber, R. H.; Bildstein, B.; Denifl, P.; Schottenberger, H. *Inorg. Chem.* **1997**, *36*, 3586.